Comparison of visible and near infrared reflectance spectroscopy for the detection of faeces/ingesta contaminants for sanitation verification at slaughter plants[d]

Yongliang Liu,[a] Kuanglin Chao,[b,*] Yud-Ren Chen,[b] Moon S. Kim,[b] Xiangwu Nou,[c] Diane E. Chan[b] and Chun-Chieh Yang[a]

[a]*Department of Biosystems and Agricultural Engineering, University of Kentucky, Lexington, KY 40546, USA*

[b]*Instrumentation and Sensing Laboratory, Henry A. Wallace Beltsville Agricultural Research Center, USDA, Building 303, BARC-East, 10300 Baltimore Avenue, Beltsville, MD 20705, USA. E-mail: Chaok@ba.ars.usda.gov*

[c]*Food Technology and Safety Laboratory, Henry A. Wallace Beltsville Agricultural Research Center, USDA, Building 201, BARC-East, 10300 Baltimore Avenue, Beltsville, MD 20705, USA*

Visible and near infrared (NIR) spectra were acquired to explore the potential for the discrimination of faeces/ingesta ("F/I") objectives from rubber belt and stainless steel ("RB/SS") backgrounds by using several wavelengths. Spectral features of "F/I" objectives and "RB/SS" backgrounds showed large differences in both visible and NIR regions, due to the diversity of their chemical compositions. These spectral distinctions formed the basis on which to develop simple three-band ratio algorithms for the classification analysis. Meanwhile, score–score plots from principal component analysis (PCA) indicated the obvious cluster separation between "F/I" objectives and "RB/SS" backgrounds, but the corresponding loadings did not show any specific wavelengths for developing effective algorithms. Furthermore, two-class soft independent modelling of class analogy models were developed to compare the correct classifications with those from the ratio algorithms. Results indicated that using ratio algorithms in the visible or NIR region could separate "F/I" objectives from "RB/SS" backgrounds with a success rate of over 97%.

Keywords: visible/near infrared spectroscopy, algorithm, poultry, faecal and ingesta contamination, sanitation and safety

Introduction

Contamination of meat and poultry with bacterial foodborne pathogens can potentially occur as a result of exposure of the animal carcass to faecal materials during or after slaughter. Microbial pathogens can be transmitted to humans by consumption of contaminated, undercooked or mishandled meat and poultry. Bacterial pathogens in food cause an estimated 76 million cases of human illnesses and up to 5000 deaths in the United States annually.[1]

To ensure a wholesome and safe meat supply to the consumers, the Food Safety Inspection Service (FSIS) of the USDA has established a policy to minimise the likelihood of bacterial pathogens on the surfaces of meat and poultry carcasses during slaughter.[2] In 1996, FSIS adopted the Pathogen Reduction, Hazard Analysis and Critical Control Points (HACCP) systems, which require all meat and poultry plants to develop written sanitation standard operating procedures to show how they will meet daily sanitation requirements.[3] This is important in reducing pathogens on poultry because unsanitary practices in slaughter plants increase the likelihood of product cross-contamination. Thus, slaughter plants are required not only to document daily records of completed sanitation standard operating procedures but also to undergo hands-on sanitation verification by FSIS inspectors.

Evaluations and inspections of sanitation effectiveness are usually performed through one or more of the following methods; organoleptic (for example, sight and feel), chemical

[d]*Mention of a product or specific equipment does not constitute a guarantee or warranty by the US Department of Agriculture and does not imply its approval to the exclusion of other products that may also be suitable.*

(for example, checking the chlorine level) and microbiological (for example, microbial swabbing and culturing of product contact surface). As poultry faeces are the most likely source of pathogenic contamination, FSIS inspectors use the established guidelines to identify faecal remains on the surfaces of equipment, utensils and walls at slaughter plants. Certainly, the inspection is both labour-intensive and prone to both human error and inspector-to-inspector variation. Therefore, researchers at the USDA Agricultural Research Service have been developing hyper- and multi-spectral reflectance and fluorescence imaging techniques for use in the detection of faecal spots on chicken carcasses and other agricultural products.[4–7] Hopefully, these imaging systems can evolve into low-cost, reliable and portable sensing devices, such as headwear goggles and binoculars. One key factor in successful applications is to use a few essential spectral bands, which should not only reflect the chemical/physical information in the samples, but also maintain successive discrimination and classification efficiency. These essential bands can be determined through a variety of analytical strategies, such as analysing the spectral difference,[8,9] performing principal component analysis[10] and stepwise linear regression.[11,12]

The objectives of this study were to determine characteristic bands in the visible and NIR regions for a set of chicken faeces and ingesta (ingested feedstuff taken by chicken and located at the beginning portion of the digestive track) as well as control samples (rubber belt and stainless steel) and to develop simple ratio algorithms for the identification of chicken faeces/ingesta ("F/I"), as objectives, from rubber belt/stainless steel ("RB/SS"), as backgrounds. Meanwhile, both principal component analysis (PCA) and two-class soft independent modelling of class analogy (SIMCA) models were used to examine the effectiveness of separation and classification. Ultimately, this research supports the development of rapid and low-cost sensing devices for *in situ* inspection of faecal/ingesta contaminants at slaughter plants for sanitation verification and poultry safety.

Materials and methods

Faecal and ingesta contaminants as well as uncontaminated background samples

A total of 221 samples, including 141 contaminants (82 faeces and 59 ingesta) and 80 uncontaminated areas (showing no visible faecal or ingesta residues) on equipment surfaces (40 samplings from shiny stainless steel and rubber belt conveyor each), was collected over an eight-day period in May of 2005 at a poultry slaughter plant. These faecal and ingesta samples were found on the steel and rubber surfaces of evisceration line equipment (manufactured by Johnson Food Equipment, Inc., Kansas City, KS, USA) during the poultry carcass processing and were identified visually by the FSIS Inspector-In-Charge. To acquire sample spectra, the samples were scanned *in situ* in the areas of the white conveyor rubber belt and the stainless steel without removing the F/I samples from the surfaces. Thus, spectra for all samples were acquired against either a rubber or stainless steel surface substrate. The size of faecal/ingesta species was from 5 mm to 10 mm in diameter (or 0.20 to 0.78 cm^2), which allowed the probe spot (*ca* 0.12 cm^2) to be fully covered with sample. For reliable detection, samples were selected with greater consideration for the size of the sample area (not less than 5 mm in one dimension) rather than for sample thickness. Every sample was visually examined on-site by a FSIS Inspector-In-Charge and categorised into one of two categories: uncontaminated (background or control) and faecal-/ingesta-contaminated.

Visible and NIR spectral measurement

Two portable spectrometers, StellarNet EPP2000-CXR and EPP2000-InGaAs (StellarNet Inc., Tampa, FL, USA), were used to collect the reflectance spectra in the visible (400–900 nm) and NIR (900–1700 nm) region, respectively. Spectral acquisitions were controlled by the manufacturer's software. Samples were illuminated by a fibre-optic light source (SL1, StellarNet Inc., Tampa, FL, USA) with a tungsten filament lamp for 300–2200 nm output. Two fibre probes (R400-7-UV/VIS and R400-7-VIS/NIR, Ocean Optics Inc., Dunedin, FL, USA) were used. These comprised seven 400 µm diameter fibres with six illumination fibres encircling one detection fibre (the numerical aperature of fibre was 0.22). A probe holder was used to maintain a consistent 45 degree angle and distance from the samples. Before collecting sample spectra, a white reference was obtained from a 7 mm thick white Spectralon panel with nearly 99% absolute reflectance (Labsphere, Sutton, NH, USA) and a dark reference was taken by pacing the optical probe 1 cm from the bottom of a black cylindrical Teflon sample cell with the light source turned off. During the measurement, the probe holder was carefully positioned so that the probe's illumination area (~ 0.12 cm^2) was not only close to the centre of the sample and the distance between sample surface and probe was about 1 cm, but also was covered fully with all F/I samples. The integration times were 300 and 150 ms for the visible and NIR measurements, respectively. Each sample spectrum was an average of 10 scans (collected at a 1 nm intervals in the visible range of 430 nm–883 nm and in the NIR range of 900 nm–1700 nm) and acquired in percentage of reflectance intensity (R). This data was converted to log ($1/R$) values and truncated into the 450–863 nm visible and 920–1680 nm NIR region for data interpretation.

Spectral processing

The data set was loaded into Microsoft Excel 2000 to execute simple algorithm analysis. It was also imported into Grams/32 to develop chemometric models (Version 5.2, Galactic Industries Corp., Salem, NH, USA). PCA on both visible and NIR spectra was performed using the PLSPlus/IQ package in Grams 32. In addition, the data representing "faeces/ingesta" ("F/I") objectives and "rubber belt/stainless steel" ("RB/SS") backgrounds were grouped and

two-class SIMCA classification models were established with spectral pre-treatments of either multiplicative scatter correction and mean centring (MSC + MC) or multiplicative scatter correction and mean centring and also Savitzky–Golay second derivative function with 11 smoothing points (MSC + MC + second derivative). One-out cross-validation was used as the validation method in both PCA and SIMCA models.

Results and discussion

Discrimination of "F/I" objectives from "RB/SS" backgrounds in the visible region

Figure 1 shows the average log(1/*R*) spectra ± one standard deviation (*SD*) envelope for faeces, ingesta, rubber belt and stainless steel samples in the visible region of 450–863 nm, which contains the colour information for the samples. The ratios of *SD* against log(1/*R*) value in average spectra at 650 nm were higher for faeces (0.61) and ingesta (0.74) than for rubber belt (0.37) and stainless steel (0.19). This was expected, because of great variations in colour and composition among faeces and ingesta samples that included a mixture of contributions from both the pigments in undigested feed and the pigments derived from the digestion process. In general, faeces ranged from yellow–orange to light brown to dark in colour compared to the ingesta which were light-green to light-yellow, while the rubber belt was white and stainless steel had a grey metallic appearance. Therefore, distinctive spectral differences should occur between faeces/ingesta ("F/I") objectives and rubber belt and stainless steel ("RB/SS") backgrounds. For example, "F/I" objectives commonly showed reduction in log (1/*R*) value from 500 nm to 600 nm, as well as at a specific band around 700 nm assignable to chlorophylls in ingesta; the rubber belt sample had a broad and weak band near 600 nm and the stainless steel did not have any bands at all in the region of 500 nm through 750 nm. Furthermore, stainless steel showed the highest log(1/*R*) intensity in the entire visible region because of its specular reflection and the rubber belt had the weakest log(1/*R*) due to its diffuse reflection.

Hence, it is of interest to examine whether "F/I" objectives and "RB/SS" backgrounds could be distinguished based on intensity difference. We developed a number of algorithms using three bands at 515, 600 and 700 nm–specifically, combinations of two- and three-band ratios and subtraction algorithms. The 515 and 700 nm bands can be assigned to carotenoids/chlorophylls in "F/I" objectives[13,14] and the 600 nm band can be related to unknown colour compounds in the rubber belt species due to ageing or contamination. We found that the three-band ratio (Q1) given in equation (1) provided the best separation power.

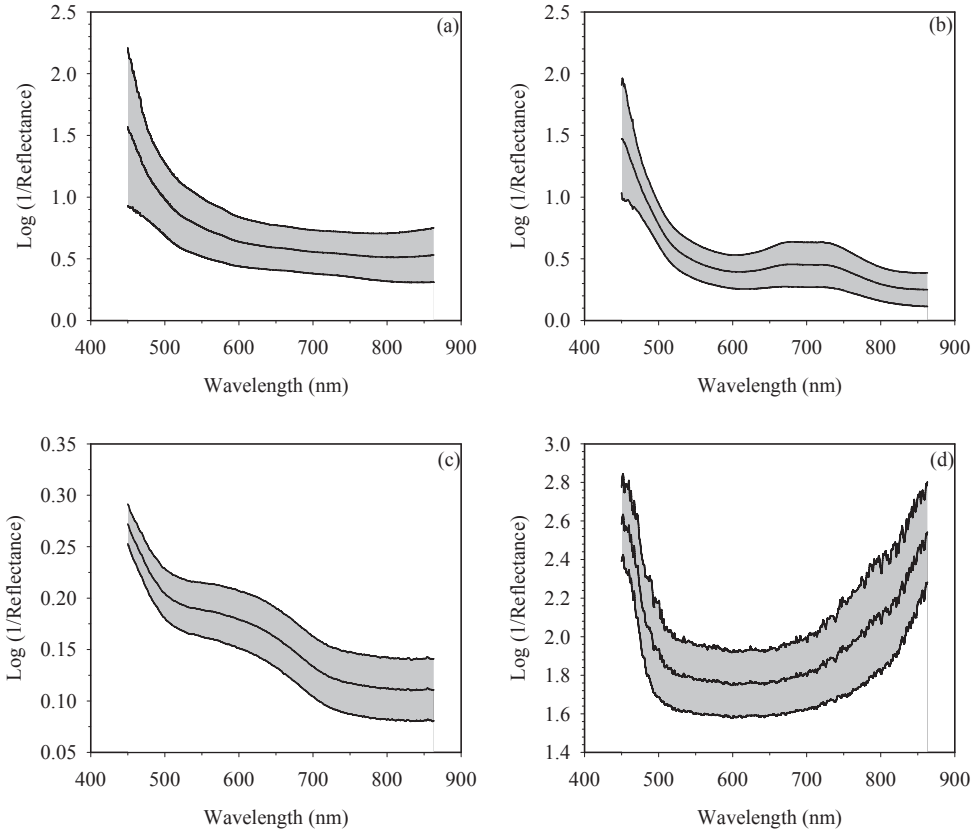

Figure 1. Average visible log (1/*R*) spectra ± one standard deviation envelope in the 450–863 nm region of (a) faeces, (b) ingesta, (c) rubber belt and (d) stainless steel samples.

$$Q1 = (A_{515\,nm} + A_{700\,nm})/A_{600\,nm} \quad (1)$$

where Q1 represents the intensity ratio and $A_{515\,nm}$, $A_{700\,nm}$ and $A_{600\,nm}$ are each a three-point average of the log (1/*R*) values at each band. For example, the $A_{515\,nm}$ value results from the mean of the log (1/*R*) intensities at 513, 515 and 517 nm.

The algorithm was applied to the visible spectral set consisting of 141 "F/I" objectives and 80 "RB/SS" backgrounds. Examination of the Q1 values suggested that Q1 values were in the range of 2.17 to 2.47 for most faeces samples, 2.27 to 3.59 for most ingesta samples, 1.65 to 1.95 for most rubber belt samples and 2.05 to 2.11 for most stainless steel samples. With a set threshold value of 2.16, i.e. a sample was classified as "F/I" objective class when Q1 > 2.16 and as "RB/SS" background otherwise, all samples but one from the rubber belt species was correctly classified (Table 1). Further smoothing (Savitzky–Golay function with two polynomial degrees and 11 smoothing points) on the raw spectra did not improve the separation results.

For comparison, PCA was used to extract useful information from the whole spectra, aiming to verify the above spectral bands. All 221 spectra were loaded into the PLSplus/IQ package in Grams/32 to perform PCA with MSC + MC spectral pre-treatments. Five principal components (PCs) accounted for 97.7% of the total variation and the first three of these PCs explained 93.5% of the variance (PC1 = 81.0%, PC2 = 8.7% and PC3 = 3.8%).

The score plot of PC1 vs PC2 provided better visualisation and is shown in Figure 2. It suggested that the stainless steel cluster could be separated easily from the other three groups by the large negative PC1 value alone and that the rubber belt samples be identified by both appropriate positive PC1 and negative PC2 scores. Meanwhile, it revealed the difficulty in the further separation between the faeces and ingesta classes. The observation indicated the potential of PCA in the classification of "F/I" objectives from "RB/SS" backgrounds.

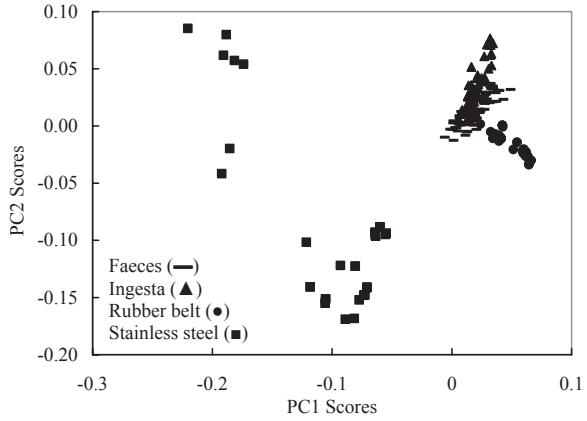

Figure 2. PC1 vs PC2 score–score plot of four sample species from the visible region, faeces (—), ingesta (▲), rubber belt (●) and stainless steel (■) classes.

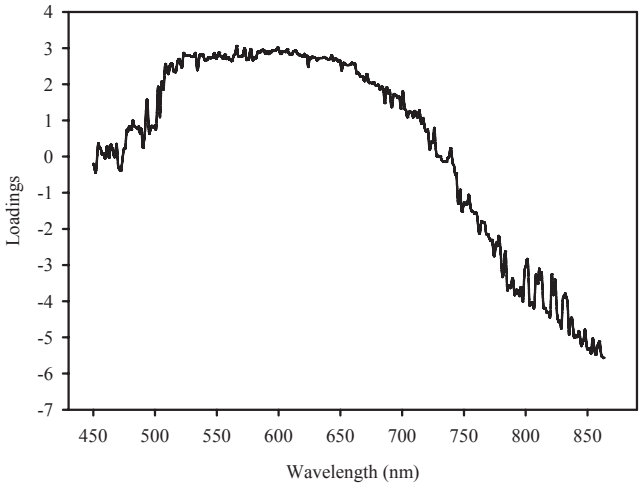

Figure 3. PC1 loadings spectrum from PCA in the visible region.

The loadings of PC1 (Figure 3), which were asymmetrical to stainless steel spectrum [Figure 1(d)] and without the characteristic peaks, showed positive loadings from 500 to 725 nm and negative loadings beyond that region. The discussion of PC2 loadings was not necessary due to lack of discrimination efficiency. Attempts to classify "F/I" objectives from "RB/SS" backgrounds, by using several bands suggested from PC1 loadings, were unsuccessful due to low correct classification rate.

Additional PCA operation on a data set only consisting of faeces, ingesta and rubber belt samples revealed that there was no clearer separation between any two of these three clusters than was already shown in Figure 2 and rubber belt samples could not be defined by a single PC value.

The PLSplus/IQ package was used to perform discriminant analysis for all 221 spectra. Ninety-five of 141 "F/I" objective spectra and 54 of 80 "RB/SS" background spectra were used for calibration development and the remaining 72 (every third sample) spectra were used for model validation. Classification models were developed in the entire region using two classes ("F/I" objectives and "RB/SS" backgrounds) and with MSC + MC pre-treatment, based on SIMCA of PCA with a Mahalanobis distance metric.[15] For "F/I" objective and "RB/SS" background classes, the optimal numbers of factors were suggested to be three and four, respectively. Applying the two-class SIMCA model to all spectra in calibration and validation sets and employing the class assignment rule of lower Mahalanobis distance, each sample was identified as being either a "F/I" objective or a "RB/SS" background. Contrary to successful classification of "F/I" objectives, a large number of "RB/SS" backgrounds were incorrectly identified (Table 1).

For comparison, the discriminant model for the same data set was developed with an additional second derivative spectral pre-treatment and the results were also summarised in Table 1. It was encouraging to observe a significant increase in classification accuracy from 68.8% to 87.3%, in which

Table 1. Ratio algorithm and two-class SIMCA model classification of faeces/ingesta ("F/I") objectives and rubber belt/stainless steel ("RB/SS") backgrouds from visible and NIR reflectance spectroscopy.

Spectral region	Model	No. of "F/I" correctly classified (total no. = 141)	No. of "RB/SS" correctly classified (total no. = 80)	Correct classification (%)[a]	Factors[b]	
					"F/I"	"RB/SS"
Visible	Q1 ratio	141	79	99.5	2.16 (threshold)	
	SIMCA / MC + MSC	140	12	68.8	4	3
	SIMCA / MC + MSC + 2nd	124	69	87.3	3	2
NIR	Q2 ratio	141	74	97.3	0.13 (threshold)	
	SIMCA / MC+MSC	136	80	97.7	6	4
	SIMCA / MC + MSC + 2nd	117	67	83.2	2	3

[a]Percentage of correct classification for a total of "F/I" objectives and "RB/SS" backgrounds
[b]Suggested optimal number of factors in calibrations for "F/I" objective and "RB/SS" background classes

"RB/SS" backgrounds were more easily identified but at significant expense of the "F/I" objectives.

Discrimination of "F/I" objectives from "RB/SS" backgrounds in the NIR region

Figure 4 shows the average log (1/*R*) spectra ± one standard deviation envelope of faeces, ingesta, rubber belt and stainless steel samples in the 920–1680 nm NIR region. Similar to the observation in the visible region, the *SD*/log (1/*R*) ratios at 1300 nm were greater for faeces (0.57) and ingesta (0.63) than for rubber belt (0.20) and stainless steel (0.16). The origins of NIR bands differ from those in the visible region and are mainly due to the (first and second) overtones and combinations of O–H, N–H and C–H stretching vibrations. Broad bands at 980, 1195 and 1450 nm are likely due to the second overtone of the O–H stretching mode of water, the second overtones of the C–H stretching modes and the first overtones of the O–H/N–H stretching modes of

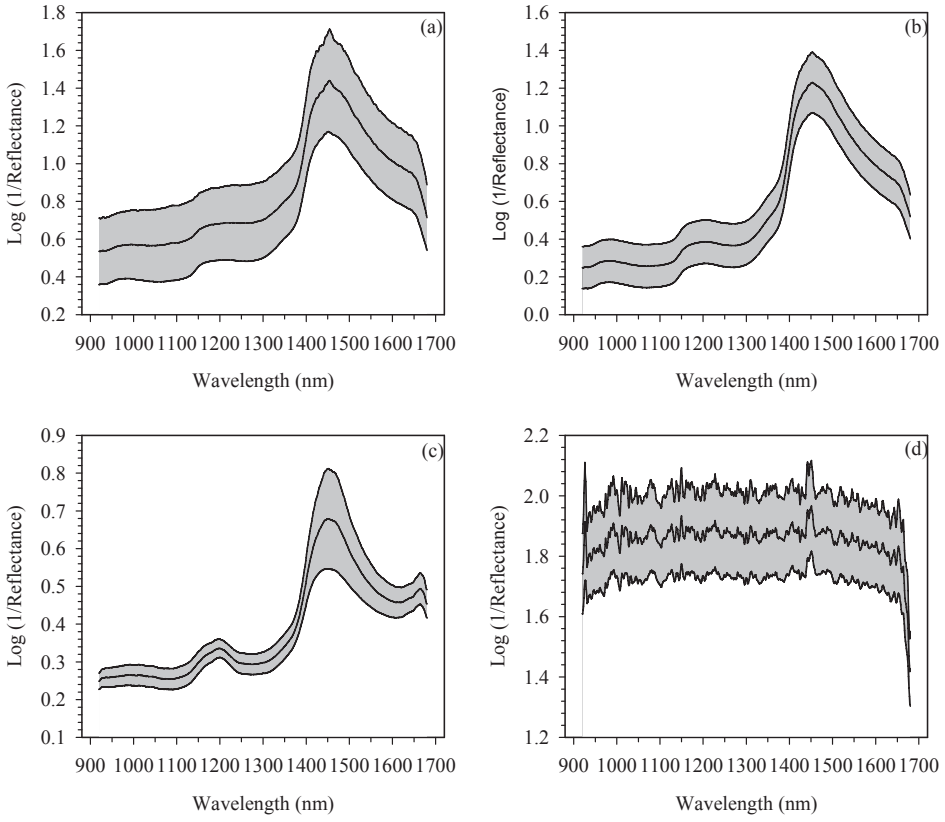

Figure 4. Average NIR log (1/*R*) spectra ± one standard deviation envelope in the 920–1680 nm region of (a) faeces, (b) ingesta, (c) rubber belt and (d) stainless steel samples.

OH/NH groups in faeces, ingesta and rubber belt samples.[16] Similar to visible spectra in Figure 1, stainless steel had the highest log (1/*R*) intensities, followed by faeces, ingesta and rubber belt samples. As expected, stainless steel showed no obvious bands except the sudden change at the start and end of the spectrum likely due to noise. Because of significant differences in chemical composition, there should be clear spectral distinction between "F/I" objectives and "RB/SS" backgrounds, such as a unique band around 1665 nm in the rubber belt spectrum and a rapid intensity decrease from 1500 to 1600 nm in the faeces and ingesta spectra. Therefore, we tested a number of algorithms utilising the 1600 and 1665 nm bands and found the three-band ratio (Q2) in equation (2) to yield promising discrimination results:

$$Q2 = (A_{1600\,nm} - A_{1665\,nm})/A_{1100\,nm} \quad (2)$$

where Q2 is the intensity ratio and $A_{1100\,nm}$, $A_{1600\,nm}$ and $A_{1665\,nm}$ each are three-point average log(1/*R*) values for individual bands centred at 1100 nm, 1600 nm and 1665 nm, respectively.

Equation (2) was used to estimate the Q2 values for a total of 221 NIR spectra consisting of 82 faeces, 59 ingesta, 40 rubber belts and 40 stainless steel samples. Analysis indicated that the Q2 values were distributed from 0.14 to 1.40 for most "F/I" objectives and from –0.04 to 0.12 for most "RB/SS" backgrounds. By setting a threshold value of 0.13, i.e. a sample was classified as "F/I" objectives when Q2 > 0.13 and as "RB/SS" backgrounds otherwise, all "F/I" objectives and 74/80 "RB/SS" backgrounds were identified correctly (Table 1).

Similarly, PCA was applied to all NIR spectra with MSC + MC spectral pre-treatments. Three PCs accounted for 98.3% of total variation, with the first two PCs accounting for over 97. 0% of the variance (PC1 = 87.0% and PC2 = 10.0%). The PC1 vs PC2 score–score plot revealed the best separation and showed that the stainless steel group was isolated, by large positive PC1 values, from the other three clusters that were close to each other. An expansion of the PC1 vs PC2 plot shown in Figure 5 suggested that most rubber belt spectra could be discriminated by appropriate negative PC1 score and, unfortunately, further separation between the faeces and ingesta groups was unlikely. Attempting to separate faeces from ingesta by exploring the combinations beyond PC1 vs PC2 was not successful, but this distinction is not significant as it is not necessary to separate them in a commercial processing plant.

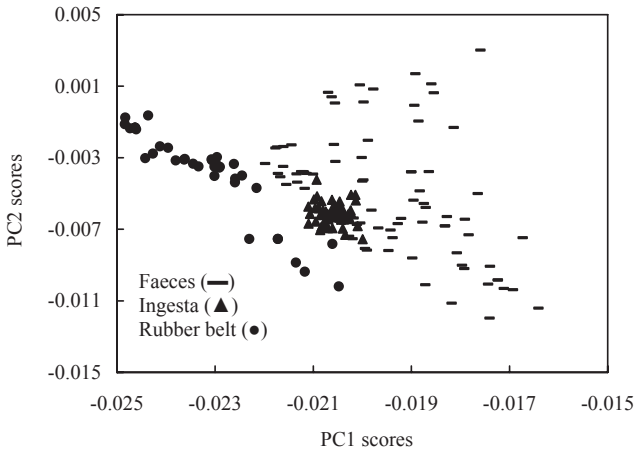

Figure 5. Expansion of PC1 vs PC2 score–score plot of four types of sample species from the NIR region, faeces (—), ingesta (▲) and rubber belt (●) classes.

The corresponding PC1 loadings, similar to the original stainless steel spectrum in Figure 4(d), revealed positive loadings from 950 to 1650 nm and negative loadings beyond the 1650 nm (not shown). Such a rapid change near 1650 nm formed the basis for the separation between faeces/ingesta/stainless steel and rubber belt groups, which was consistent with earlier spectral analysis.

Next, two-class classification models were developed for all spectra in the entire NIR region. Assignment of NIR spectra in both calibration and validation sets was exactly the same as that of visible spectra. Application of the two-class SIMCA model to NIR spectra revealed an excellent separation (Table 1). Meanwhile, the SIMCA model with MSC + MC + 2nd derivative pre-treatment resulted in a decrease in classification rate from 97.7% to 83.2% for both "F/I" objectives and "RB/SS" backgrounds.

Comparison of the results shown in Table 1 suggested that classification from the simple three-band ratio algorithm in the visible region was much better than that from the two-class SIMCA models and the statistics from the ratio algorithm in the NIR region were nearly as effective as those from the SIMCA models. Generally, the ratio algorithm in the visible region yielded slightly better separation rates than the one in the NIR region, but both reached over 97% accuracy. The results suggested the importance of three visible or NIR bands in the detection of "F/I" objectives on a rubber belt and stainless steel surface. Obviously, the three-band approach from either visible or NIR region is very attractive and promising in the design of low-cost and portable sensing devices for the verification of sanitation processes at slaughter plants. Certainly, the selection of visible or NIR bands depends on many factors, such as final product cost and *in situ* performance.

Conclusions

The study presented a direct analysis of visible and NIR spectra for the classification of "F/I" objectives from "RB/SS" backgrounds. Spectral differences in both visible and NIR regions revealed a number of significant bands, which were used to develop simple three-band ratio algorithms for discriminant analysis. The results showed that the three-band-based algorithms could classify "F/I" objectives from "RB/SS" backgrounds with a success of over 97%, which was at least the same accuracy as those from the two-class SIMCA models. Meanwhile, PCA was performed on both

spectral sets and the score–score plot showed a clear separation between "F/I" objectives and "RB/SS" backgrounds. However, the optimal loadings did not provide any specific characteristic bands that could further improve the classification rate. The finding of three visible or NIR bands is most promising in the development of a simple goggle and binocular sensing system for *in situ* inspection of faecal and ingesta contaminants at slaughter plants.

References

1. P.S. Mead, L. Slutsker, V. Dietz, L.F. McCaig, J.S. Bresee, C. Shapiro, P.M. Griffin and R.V. Tauxe, *Emerg. Infect. Dis.* **5,** 607 (1999).
2. Enhanced poultry inspection. Proposed rule. Fed. Reg. 59:35659. USDA, FSIS, Washington DC, USA (1994).
3. Pathogen reduction, hazard analysis and critical control point (HACCP) systems. Final Rule. Fed. Reg. 61:28805-38855. USDA, FSIS, Washington DC, USA (1996).
4. A.M. Lefcourt, M.S. Kim and Y.R. Chen, *Computers and Electronics in Agriculture* **48,** 63 (2005).
5. K.C. Lawrence, W.R. Windham, B. Park and R.J. Buhr, *NIR news* **12,** 1 (2001).
6. M.S. Kim, A.M. Lefcourt, K. Chao, Y.R. Chen, I. Kim and D.E. Chan, *Trans. ASAE* **45,** 2027 (2002).
7. P.M. Mehl, Y.R. Chen, M.S. Kim and D.E. Chan, *J. Food Eng.* **61,** 67 (2004).
8. Y. Liu, W.R. Windham, K.C. Lawrence and B. Park, *Appl. Spectrosc.* **57,** 1609 (2003).
9. Y. Liu, Y.R. Chen, C.Y. Wang, D.E. Chan and M.S. Kim, *Appl. Spectrosc.* **59,** 78 (2005).
10. W.R. Windham, K.C. Lawrence, B. Park and R.J. Buhr, *Trans. ASAE* **46,** 747 (2003).
11. W.R. Windham, D.P. Smith, B. Park, K.C., Lawrence and P.W. Feldner, *Trans. ASAE* **46,** 1733 (2003).
12. P. Williams and K. Norris, *Near-Infrared Technology in the Agricultural and food Industries*. American Association of Cereal Chemists, St Paul, MN, USA (2001).
13. F.J. Framcis and F.M. Clydesdale, *Food Colorimetry: Theory and Application.* Chapman & Hall, New York, USA (1975).
14. L.P. Vernon and G.R. Seely, *The Chlorophylls*. Academic Press, New York, USA (1966).
15. *PLSplus/IQ for GRAMS/32 and GRAMS/386*. Galactic Industries Corp., New Hampshire, USA, (1996).
16. B.G. Osborne, T. Fearn and P.H. Hindle, *Practical near infrared spectroscopy with application in food and beverage analysis*, 2nd Edn. Longman Scientific & Technical, Harlow, Essex, UK, (1993).

Received: 25 January 2006
Revised: 5 August 2006
Accepted: 29 August 2006
Web Publication: 21 November 2006